Synthetic Biology, 2018, 3(1): ysy005

doi: 10.1093/synbio/ysy005
Research Article

Simultaneous monitoring of transcription and translation in mammalian cell-free expression in bulk and in cell-sized droplets

Shue Wang[1], Sagardip Majumder[1], Nicholas J. Emery[1,2], and Allen P. Liu[1,3,4,5,*]

[1]Department of Mechanical Engineering, University of Michigan, Ann Arbor, MI, USA, [2]Department of Biomedical Engineering, Boston University, Boston, MA, USA, [3]Department of Biomedical Engineering, University of Michigan, Ann Arbor, MI, USA, [4]Cellular and Molecular Biology Program, University of Michigan, Ann Arbor, MI, USA and [5]Biophysics Program, University of Michigan, Ann Arbor, MI, USA

*Corresponding author: E-mail: allenliu@umich.edu

Abstract

Transcription and translation are two critical processes during eukaryotic gene expression that regulate cellular activities. The development of mammalian cell-free expression (CFE) systems provides a platform for studying these two critical processes *in vitro* for bottom-up synthetic biology applications such as construction of an artificial cell. Moreover, real-time monitoring of the dynamics of synthesized mRNA and protein is key to characterize and optimize gene circuits before implementing in living cells or in artificial cells. However, there are few tools for measurement of mRNA and protein dynamics in mammalian CFE systems. Here, we developed a locked nucleic acid (LNA) probe for monitoring transcription in a HeLa-based CFE system in real-time. By using this LNA probe in conjunction with a fluorescent reporter protein, we were able to simultaneously monitor mRNA and protein dynamics in bulk reactions and cell-sized single-emulsion droplets. We found rapid production of mRNA transcripts that decreased over time as protein production ensued in bulk reactions. Our results also showed that transcription in cell-sized droplets has different dynamics compared to the transcription in bulk reactions. The use of this LNA probe in conjunction with fluorescent proteins in HeLa-based mammalian CFE system provides a versatile *in vitro* platform for studying mRNA dynamics for bottom-up synthetic biology applications.

Key words: mammalian cell-free expression; *in vitro* transcription and translation; single-emulsion droplets

1. Introduction

The two fundamental cellular activities in gene expression are transcription and translation (TX–TL). It is well appreciated that these two events play central roles in regulating cellular functions and determining cell fate (1). Although TX–TL have been studied extensively in recent years (2–4), simultaneous detection of mRNA and protein expression is still challenging. Recently, single molecule techniques have been applied in living cells that use multiepitope tags and fluorescently labeled antibodies or protein probes to track TX–TL in real-time (5, 6). These approaches rely on the concentration of fluorescence from a diffuse background into individual puncta, and mRNAs are monitored by MS2 stem loops that limit the potential for multiplexing. In recent years, the emergence of cell-free synthetic biology has opened up opportunities for studying complex cellular activities *in vitro*, i.e. TX–TL (7–9). This powerful technology allows biological networks to be engineered in a more controllable and less complex environment, which allows rapid prototyping of newly designed gene circuits before implementing them in living cells. Meanwhile, cell-free expression

Submitted: 6 November 2017; **Received (in revised form):** 24 March 2018; **Accepted:** 17 April 2018

(CFE) systems have been developed over the last few decades and have become a versatile tool to study *in vitro* reactions. Numerous platforms are now commercially available or can be readily prepared in laboratories (10–13). For example, Shin and Noireaux have established an *Escherichia coli* CFE system using endogenous sigma factors for rapid testing of synthetic gene circuits (10, 11). PURExpress (New England Biolabs) and Expressway (Thermo Fisher Scientific) are two commercialized CFE systems. The dynamics and behaviors of gene circuits, including multistage cascades, gates, oscillators and negative feedback loops have been investigated using an *E. coli*-based protein synthesis system (10, 14). Moreover, vesicles containing *E. coli*-based cell-free reactions have been established as an artificial cell platform (15, 16). In contrast to *E. coli*-based systems, mammalian CFE systems present greater complexity and are less well-understood; however, mammalian CFE systems have increasingly gained researchers' interests due to their ability to carry out post- and co-translational modifications (17, 18). A HeLa-based CFE system was developed by the Imataka group and implemented in our group for the construction of artificial cells (19, 20). In this system, HeLa-based lysate is supplemented with a translation regulator to enhance the efficiency of translation and uses T7 RNA polymerase for transcription. This versatile mammalian CFE system has been utilized to express both soluble and membrane proteins in double emulsion templated vesicles (17).

In CFE systems, dynamics of mRNA and protein synthesis are key parameters that are needed to optimize the performance of gene circuits. Thus, it is important to track TX–TL dynamics to acquire temporal information of synthesized mRNA and protein. It has been shown that synthesized protein can be detected by the use of fluorescent reporter protein (11, 19, 21, 22). For RNA, spinach and broccoli aptamers were recently developed to monitor RNA activities in *E. coli*-based CFE, bacteria and mammalian cells (23–26). These RNA aptamers can bind to certain small organic dyes whose fluorescence is switched on in the presence of the RNA aptamer. An alternative approach for mRNA detection is the usage of locked nucleic acid (LNA) probes which are designed to bind specific target sequences, instead of using a genetically encoded RNA aptamer that is fused to RNA of interest. LNA probes have been demonstrated for spatiotemporal mRNA or microRNA detection at the single-cell level and were also applied to mRNA profiling in native tissue (27–29). Furthermore, simultaneous detection of mRNA and protein expression in non-mammalian CFE systems have been reported by several groups. Niederholtmeyer *et al.* (30) have developed a binary probe to monitor mRNA dynamics in a *E. coli*-based CFE, and van Nies and Danelon have demonstrated tracking of mRNA and protein synthesis dynamics by inserting a spinach aptamer into the 3′-UTR of YFP in a minimal CFE system (31, 32). However, previous monitoring of TX–TL dynamics was mainly performed in bulk in *E. coli*-based cell-free systems. Although Danelon and colleagues have applied their mRNA detection system in liposome-confined reactions (31), temporal dynamics of mRNA and protein expression were not investigated. Simultaneous detection of mRNA and protein dynamics in mammalian CFE systems in bulk and in encapsulated microenvironments have not been reported to date.

In this work, we developed an LNA probe for real-time detection of transcription and simultaneously monitored translation dynamics in a mammalian CFE system in bulk and in cell-sized single-emulsion droplets. A HeLa-based CFE system was prepared in-house, and this has been used in our group for several applications (20, 33–35). An LNA probe was designed to detect the mRNA sequence of green fluorescent protein (GFP). The performance of this LNA probe was first characterized and optimized *in vitro*. The mRNA and protein dynamics were monitored simultaneously with different concentrations of DNA plasmid in bulk CFE reactions. In order to monitor the dynamics of mRNA and protein synthesis in cell-sized droplets, a microfluidic device was used for the generation of cell-sized single-emulsion droplets. By encapsulating mammalian CFE reactions and an LNA probe, we investigated the mRNA and protein expression dynamics in cell-sized single-emulsion droplets. The LNA probe and HeLa-based CFE system, together with a single-emulsion droplet generation microfluidic device, provide an efficient and versatile platform for investigating and characterizing gene circuits in the context of artificial cells.

2. Materials and methods

2.1 LNA probe design

The LNA probe consists of alternating LNA/DNA monomers with a 21-base oligonucleotide. In order to design LNA probe to detect mRNA expression in CFE, the minimum free energy structure of the mRNA was computed using RNAFold web server. The target sequence can thus be selected and optimized by checking loop specificity. The LNA probe sequence is complementary to the loop region of the target mRNA structure. The binding affinity and specificity were optimized using mFold server and NCBI Basic Local Alignment Search Tool (BLAST) database. To acquire fluorescence detection, the LNA probe was labeled with a fluorophore (Texas Red) at the 5′ end. The quencher is a 10-base LNA/DNA oligonucleotide that is complementary to the 5′ end of LNA probe. The quencher strand was labeled with Iowa Black RQ on the 3′ end to quench the red fluorescence of the LNA probe. The LNA probe was synthesized by Exiqon Inc. The quencher sequence and corresponding target DNA sequences were synthesized by Integrated DNA Technologies Inc. (IDT).

2.2 Double-stranded LNA probe preparation

The LNA probe and quencher were initially prepared in 1× Tris-ethylenediaminetetraacetic acid (EDTA) buffer (pH 8.0) at a concentration of 100 nM. The LNA probe and quencher were mixed and incubated at 95°C for 5 min in a pre-heated heat block and cooled down to 32°C over the course of 2 h. The fluorescent probe and quencher strand were prepared in a number of different ratios to optimize the signal-to-noise ratio. The quenching efficiency was evaluated by measuring fluorescence intensity using a fluorescence microplate reader (BioTek, Synergy 2). The optimized LNA probe/quencher mixer was then ready to be used for mRNA detection in CFE reactions.

2.3 Preparation of HeLa-based cell-free expression system

HeLa-based CFE system includes HeLa lysate, truncated GADD34, T7 RNA polymerase, mix 1 and mix 2 solutions. The HeLa lysate was prepared from spinner-cultured HeLa S3 cells (ATCC Inc.). The detailed preparation steps can be found in a previously published work (19). Briefly, HeLa S3 cells were cultured in suspension using minimal essential medium eagle medium (SMEM) with Joklik modification without calcium, at an initial concentration of 1–2 $\times$ 10^5 cells/ml. Cells were harvested and lysed when the concentration reached 7–8 $\times$ 10^5 cells/ml after 4-5 days of culture. The harvested HeLa lysate was aliquoted and stored at −80°C. GADD34 and T7 RNA polymerase were prepared with the stock concentration of 2.3 and 5 mM,

respectively. Mix 1 is a buffer prepared with 27.6 mM $Mg(OAc)_2$, 168 mM 4-(2-hydroxyethyl)-1-piperazineethanesulfonic acid (K-HEPES pH 7.5). Mix 2 is a solution which was prepared with the following reagents: 12.5 mM ATP, 8.36 mM GTP, 8.36 mM CTP, 8.36 mM UTP, 200 mM creatine phosphate, 7.8 mM K-HEPES (pH 7.5) and 0.6 mg/ml creatine kinase. The pT7-CFE-GFP plasmid was prepared by cloning GFP protein into pT7-CFE-CHis vector (Thermo Fisher Scientific). The inserted GFP sequence can be found in Supplementary Table S2.

2.4 Sample preparation for CFE reactions

The HeLa-based CFE reactions were prepared by mixing the different components together. First, HeLa lysate, truncated GADD34, and mix 1 solution were mixed and incubated at 32°C for 10 min in a pre-heated water bath. The rest of the components including T7 RNA polymerase, mix 2 solution, plasmid DNA and LNA probe/quencher were mixed together. Details of sample preparation can be found in our previous work (20). The samples were prepared in triplicate with a final volume of 10 µl per sample. All the fluorescence measurements were taken in 96 well clear v-bottom polypropylene microplates using a fluorescence microplate reader (BioTek, Syngery 2). The fluorescence intensity was measured at the excitation wavelengths of 485 and 590 nm and emission wavelengths of 525 and 617 nm at every 3 min interval for 4 h at 32°C.

2.5 Calibration of GFP standard curve

A set of GFP standards was produced by serial dilution of purified GFP in a solution containing 12.5 mM Tris-HCl, 150 mM NaCl and 50% glycerol (pH 7.5). A standard curve was produced by measuring the fluorescence of varying concentrations of GFP in a microplate reader at 32°C using excitation and emission wavelengths of 485 and 525 nm, respectively. The serial dilutions and fluorescence measurements were performed in triplicate, and the average fluorescence reading for each concentration was obtained. A linear regression through these average values was used to approximate absolute GFP concentrations in CFE experiments.

2.6 Computational model of transcription-translation dynamics

A computational model was developed to study the dynamics of mRNA and protein expressions. In this model, mRNA is synthesized at a rate of k_{tr} and degraded at a rate of d_{tr}. First, the mRNAs are translated into immature protein at a rate of k_{tl} with a degradation rate of d_{tl}. The immature protein then folds and forms mature functional protein at a rate of k_{mp} and degrades at a rate of d_{mp}. The kinetics of the synthesis process of mRNA and protein can be described by the following differential equations (1–3).

$$dm/dt = k_{tr}[D] - d_{tr}[m] \quad (1)$$

$$dp/dt = k_{tl}[m] - k_{mp}[p] - d_{tl}[p] \quad (2)$$

$$dp_m/dt = k_{mp}[p] - d_{mp}[p_m] \quad (3)$$

Here, dm/dt, dp/dt and dp_m/dt are the rates of change of mRNA $[m]$, immature protein $[p]$ and mature protein $[p_m]$. k_{tr}, k_{tl} and k_{mp} are the first order transcription rate, translation rate and protein maturation rate, respectively. d_{tr}, d_{tl} and d_{mp} are the mRNA, immature protein and mature protein first order degradation rates. Since there is no degradation observed in our CFE results, the degradation rates are set to zero ($d_{tr} = d_{tl} = d_{mp} = 0$) in this model. As indicated in Equation (1), the mRNA level $[m]$, depends on the transcription rate. The protein level depends on the number of mRNAs and translation rate. The transcription rate and translation rate were determined based on the experimental data in bulk reactions. The mRNA and protein levels were first quantified by measuring fluorescence intensity relative to standard curves. The simulation curves were then fitted by adjusting the transcription rate k_{tr} and translation rate k_{tl}.

2.7 Microfluidic device fabrication

The microfluidic device for single-emulsion generation consisted of a polydimethylsiloxane (PDMS) microchannel layer with two inlets channels, one outlet channel and a bottom glass slide. The PDMS microfluidic channel layer was fabricated using soft lithography. The measured outer phase and inner phase channel dimensions are 80 µm wide, 64 µm high and 50 µm wide, 64 µm high, respectively. The PDMS was mixed at a 1:10 curing agent-to-elastomer base ratio and casted onto a positive mold made of patterned SU-8, and then cured at 80°C for 2 h. The PDMS layer was then bonded permanently to a microscope glass slide following oxygen plasma treatment.

2.8 Preparation of water-in-oil single-emulsion droplets

Mineral oil with the surfactant Span 80 (2% v/v) was prepared in 1 ml syringe for outer phase solution. HeLa-based CFE solutions with DNA template and LNA probe/quencher were mixed together to make the inner phase solution. Two syringe pumps (New Era Pump Systems, NE-500) were utilized to pump oil and CFE solutions into the outer and inner phase channels of the microfluidic device for the formation of single emulsions. The flow rates were set to 500 and 300 µl/h, respectively. The generated single emulsions flowed through the collection channel and were then collected in a collection tube.

2.9 Imaging

The generated single-emulsion droplets were collected in a 1.5 ml microcentrifuge tube. Before imaging, the droplets were diluted in mineral oil at the ratio of 1:10. The diluted droplets with the volume of 30 µl were added to a self-made coverslip imaging chamber and sealed with VALAP (1:1:1 of vaseline, lanolin and paraffin). The fluorescence images of single-emulsion droplets were captured using an Olympus DSU-IX81 spinning disc confocal microscope equipped with an EMCCD camera (iXon X3, Andor). The images were acquired separately under the same exposure time of 500 ms for both channels (GFP and Texas Red) at 1, 3 and 5 h.

2.10 Statistical analysis

Data are presented as mean ± SEM. All the measurements were conducted in triplicate and repeated at least three times independently. Student's t-tests were performed to analyze statistical significance between experimental groups.

3. Results and discussions

3.1 Design of the LNA probe for dynamic mRNA monitoring

In order to detect TX–TL dynamics, a novel platform was designed that consisted of a HeLa-based CFE system and a double-stranded LNA probe. As shown in Figure 1A, the

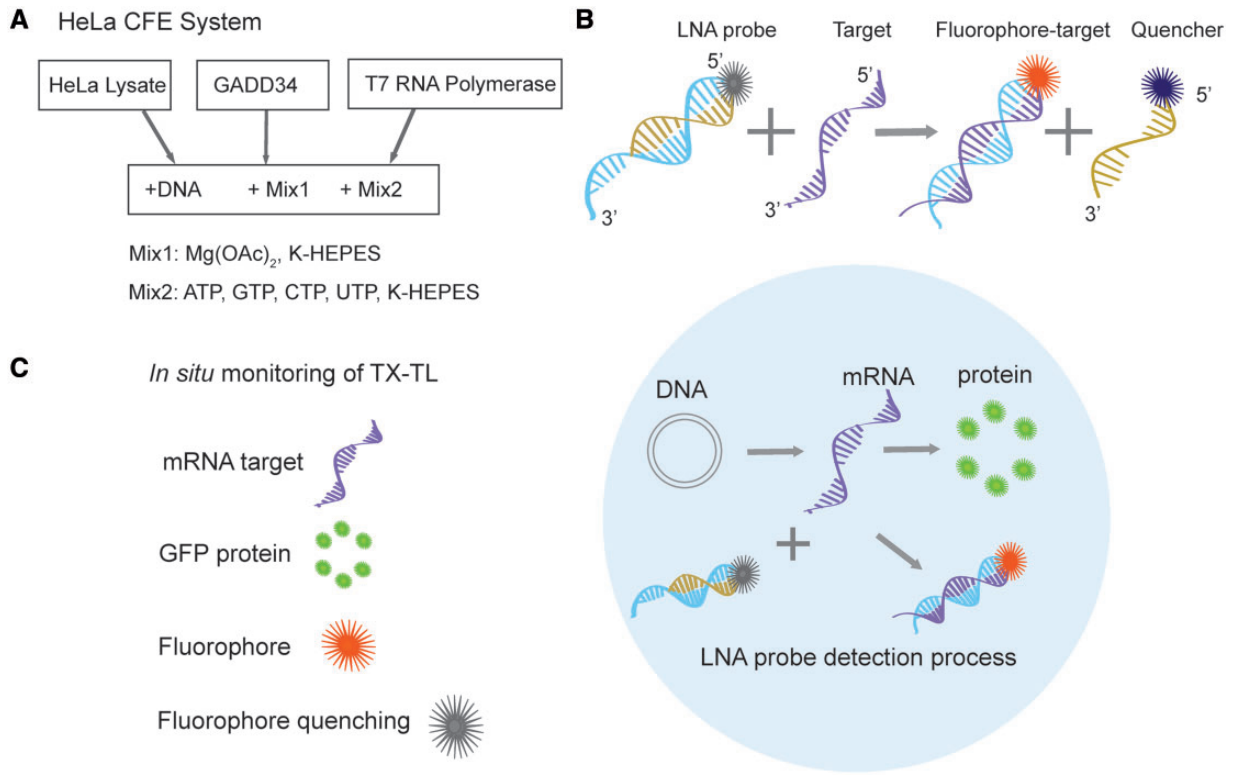

Figure 1. Illustration of real-time detection of TX–TL dynamics using HeLa-based CFE system and double-stranded LNA probe. (**A**) Components of HeLa-based CFE system. (**B**) Working principle of double-stranded LNA probe for mRNA detection. (**C**) Illustration of monitoring TX–TL dynamics in cell-sized droplets.

HeLa-based CFE system is composed of HeLa lysate, purified truncated GADD34 and T7 RNA polymerase to enable single step TX–TL reactions. GADD34 dephosphorylates eukaryotic initiation factor 2a to promote translation reaction (36). HeLa lysate was prepared from spin-cultured HeLa S3 cells. This HeLa-based CFE system has been optimized and demonstrated to express GFP and other proteins over many hours (20), which provides an effective platform to test and optimize gene circuits. To achieve real-time monitoring of transcription dynamics, a double-stranded LNA probe was designed to monitor GFP transcription dynamics in HeLa-based CFE. This probe includes two strands of oligonucleotides, a detecting strand labeled with a fluorophore (Texas Red) and a quenching strand labeled with Iowa Black to quench the fluorescence signal in the absence of a target (Supplementary Table S1). The LNA probe is a 21-base oligonucleotides sequence with alternating LNA/DNA monomers. The LNA nucleotides are modified DNA nucleotides with higher thermal stability and specificity. The probe was designed based on the specific target sequence. The detecting strand binds to the quenching strand spontaneously due to a high binding affinity (Supplementary Table S1). The large difference in binding free energy between LNA probe to mRNA versus LNA probe to quencher means that once the LNA probe binds to the target mRNA, the binding is stable against rebinding of the quencher. In the presence of a target sequence, the LNA probe is thermodynamically displaced from the quenching strand and a fluorescence signal is observed (Figure 1B). Taken together, the HeLa-based CFE system and double-stranded LNA probe enable simultaneous monitoring of TX–TL dynamics by measuring fluorescence intensity over time. Single-emulsion droplets can be generated as a model of artificial cells by encapsulating the HeLa-based CFE system and the double-stranded LNA probe (Figure 1C). Thus, TX–TL dynamics in cell-sized droplets can be studied.

3.2 Characterization of double-stranded LNA probe

In order to optimize the double-stranded LNA probe for monitoring transcription activities in CFE system and in artificial cells, we first characterized the optimal quencher-to-fluorophore ratio. To minimize the background caused by free fluorophore during reactions, the optimal quencher-to-probe ratio was determined by adjusting the quencher concentrations. The fluorophore concentration was set to 100 nM, and the quencher concentrations were then adjusted such that the quencher-to-probe ratio ranged from 0.5 to 10. Figure 2A shows the fluorescence intensity levels measured at different quencher-to-probe ratios. The fluorescence intensity of fluorophore decreased as the quencher concentration increased. Quencher-to-probe ratios were set at 0.5, 1, 1.5, 2, 3, 4, 5 and 10, which resulted in quenching efficiencies of 41.8%, 81.5%, 95.7%, 96.4%, 97.2%, 97.3%, 98.1% and 98.3%, respectively. This result indicates that the intensity of the fluorophore was effectively quenched to a low level (about 3% of the maximum value) at a quencher-to-fluorophore ratio of 2:1. Further increases in the quencher concentration did not further reduce the fluorescence intensity significantly (up to a ratio of 10:1). This is consistent with previously reported theoretical equilibrium analysis and experimental results (37). Thus, the quencher-to-probe ratio was set at 2:1 for all subsequent studies. The dynamic range of detectable target concentrations was estimated experimentally by varying the concentration of a single stranded DNA target oligonucleotide while holding the probe concentration at 100 nM (Figure 2B). The titration curve shows a sigmoid shape and exhibits a large dynamic range for quantifying the target

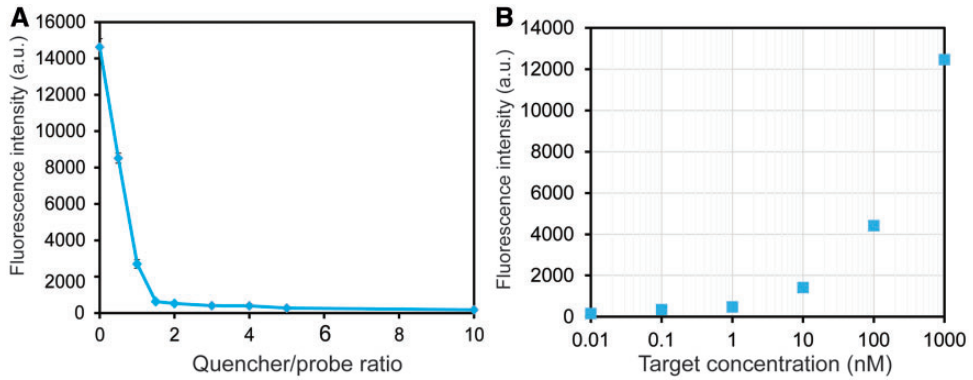

Figure 2. Characterization of double-stranded LNA probe. (**A**) Calibration of the quencher-to-probe ratio measured on a fluorescence plate reader. (**B**) Detection dynamic range of the double-stranded LNA probe was determined using 100 nM probe and varying concentrations of target strand. Data are expressed as mean ± SEM. Experiments were repeated three times independently.

concentration (from 2 to 1000 nM). This confirmed that a probe concentration of 100 nM provides a sufficiently large dynamic range, and this probe concentration was used in all subsequent experiments. Furthermore, the stability of the LNA probe was evaluated at different pH values, ranging from 6 to 10 (Supplementary Figure S1A), and also over time for up to 400 min (Supplementary Figure S1B). These results indicate that the stability of double-stranded LNA probe is not affected at different pH values and that the probe remains stable over several hours. Moreover, we examined the background fluorescence intensity of the double-stranded LNA probe with each CFE component and observed some non-specific de-quenching of LNA probe in HeLa lysate (Supplementary Figure S2A; an increase from 200 to 700 in relative fluorescence unit). This increase was a fraction (~12%) of the specific fluorescence de-quenching when the target was present (Figure 2B, when the target concentration is 100 nM). The rest of the components (T7, GADD, Mix 1, Mix 2 and DNA) did not contribute to the background fluorescence intensity of the probe (Supplementary Figure S2A). As expected, none of the components contributed to the green fluorescence channel with or without the LNA probe (Supplementary Figure S2B). In order to rule out artifacts from the lysate, we added protein synthesis inhibitor cycloheximide (CHX) to the reactions (Supplementary Figure S3). The synthesized GFP was significantly inhibited with CHX. In contrast, the mRNA production was slightly reduced by CHX, which is consistent with previously reported results (38). We have also conducted experiments without added T7 RNA polymerase and acquired mRNA and protein fluorescence under identical conditions. There were no changes in both fluorescence channels over the entire time course (not shown). All these results indicate that the fluorescence of the probes and GFP were specific and not due to photophysics or other effects from the lysate. Since protein expression can be detected as early as 45 min (due to maturation of GFP) in HeLa-based CFE system, the TX–TL dynamics were monitored for 4 h in our study.

3.3 Simultaneous detection of TX–TL dynamics in a HeLa-based CFE system

To demonstrate the capability of the LNA probe for simultaneous detection of TX–TL dynamics, mRNA and protein expression levels in a HeLa-based CFE system were monitored on a fluorescence plate reader over 4 h sampling every 3 min. First, we confirmed that the LNA probe did not affect GFP expression dynamics (using pT7-CFE-GFP, Supplementary Table S2) in HeLa-based CFE (Supplementary Figure S4A and B). The TX–TL dynamics were quantified by measuring fluorescence intensity with the excitation/emission wavelength of 590/617 nm (red channel) for the LNA probe and 485/525 nm for GFP (green channel), respectively. Without the LNA probe, there was no fluorescence signal detected in CFE when excited at 590 nm (Supplementary Figure S4A), as expected. As shown in Supplementary Figure S4B, the fluorescence intensity of synthesized GFP was the same with and without the LNA probe, indicating that GFP expression dynamics in CFE was not affected by the presence of LNA probe. This suggests that the LNA probe does not hinder translation by sequestering mRNA. Next, we proceeded to investigate TX–TL dynamics using the LNA probe in conjunction with GFP fluorescence by monitoring HeLa-based CFE reactions in both the red channel and green channel. When LNA probe and DNA plasmid were added to the CFE, mRNA and protein were synthesized and can be readily measured and quantified. Three different conditions were tested: CFE alone as a negative control, CFE with LNA probe, CFE with LNA probe and DNA plasmid. The synthesized mRNA and protein concentrations were calculated according to calibration curves shown in Figure 2B and Supplementary Figure S5. The background fluorescence levels of CFE in both channels over time were minimal (Supplementary Figure S6A and B). In order to test whether HeLa lysate has an effect on template DNA (e.g. through DNAase activity), we pre-incubated HeLa lysate with pT7-CFE-GFP plasmid for 4 h and measured the synthesized GFP compared to a control without pre-incubation. After a 4-h incubation, the rest of the components, including T7 RNA polymerase, GADD34 and mix 1 and mix 2 solutions were added. There were no significant differences in synthesized GFP with and without pre-incubation (Supplementary Figure S7), which suggests that HeLa lysate does not have a significant influence on the stability of DNA template.

After 4 h of incubation of the complete reactions, the synthesized mRNA concentrations obtained were 20.2 nM, 50.7 nM, 109.2 nM and 159.5 nM at DNA concentrations of 1 nM, 2 nM, 3 nM and 5 nM, respectively. The synthesized protein concentrations obtained were 13.2 nM, 72.2 nM, 143.5 nM and 199.8 nM with the DNA concentrations of 1 nM, 2 nM, 3 nM and 5 nM, respectively (Figure 3A and B). While GFP mRNA was produced almost immediately and could be detected by LNA probe, GFP was not detected until almost 45 min (due to GFP maturation) after the reactions began. Thus, monitoring protein translation in our system is not in real-time. The monotonic increases of both mRNA and protein were non-linear with respect to both time and DNA concentration. These results can be contrasted with

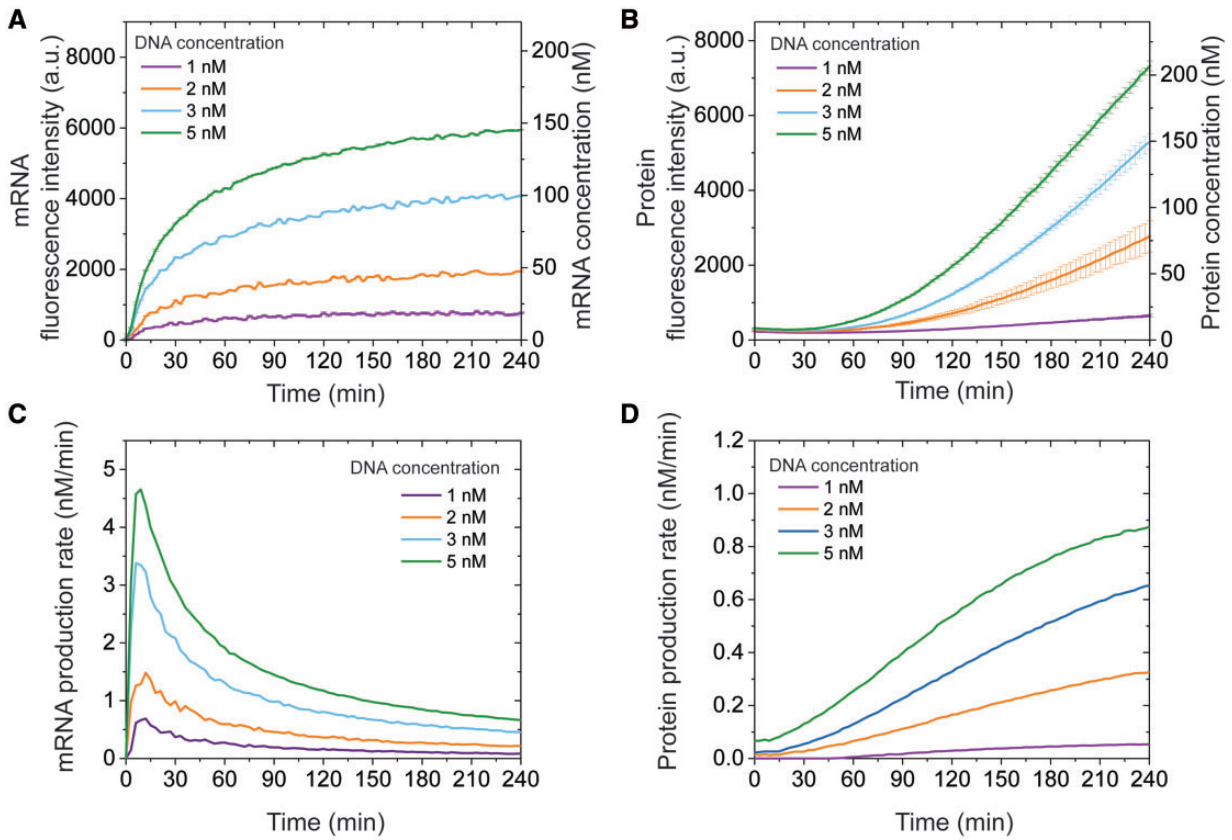

Figure 3. Simultaneous monitoring of mRNA and protein synthesis dynamics in HeLa-based CFE. (**A**) mRNA synthesis dynamics at different plasmid DNA concentrations. (**B**) Protein synthesis dynamics at different plasmid DNA concentrations. (**C**) mRNA production rate in CFE at different DNA concentrations calculated from (A). (**D**) Protein production rate in CFE at different DNA concentrations calculated from (B). The concentration of LNA probe was 100 nM for all the experiments and reaction conditions are described in Section 2. Experiments were repeated three times independently. Data are expressed as mean ± SEM.

previous studies of mRNA and protein dynamics in *E. coli*-based CFE systems, in which the mRNA concentration reached a peak at 100 min and gradually decreased to a low level after 500 min while protein concentration continued to increase (39). The precise origins of these differences are not immediately clear; however, the results highlight the need for more extensive characterization of mRNA and protein expression dynamics in mammalian CFE systems, which may not mirror those of bacterial systems. A computational model was developed that qualitatively captured the TX–TL dynamics (Supplementary Figure S8A–C). The mRNA and protein production rates were extrapolated from the experimental mRNA and protein expression dynamics (Figure 3C and D). The mRNA production rate was high at the beginning, peaked at ~10–15 min, and decreased after 30 min of reaction. It should be noted that the transcription dynamics observed here may be specific to HeLa CFE systems utilizing T7 RNA polymerase, which increases transcription rate substantially relative to endogenous transcription machinery. A T7 system was used here because of the widespread adoption of T7 promoter in many CFE applications. Compared to the transcription rate, the protein production rate gradually increased during the same period and began to level off after 4 h (Figure 3D). These results indicated that in eukaryotic CFE, TX–TL are separated in time and follow different dynamics.

3.4 Monitoring TX–TL in single-emulsion droplets

In order to visualize TX–TL dynamics in cell-sized single-emulsion droplets, a microfluidic device was designed and fabricated for the encapsulation of HeLa-based CFE and LNA probe. Microfluidic techniques have been widely developed and applied to different fields including single-cell analysis, cancer metastasis and angiogenesis over the last two decades (40–43). However, microfluidic encapsulation of bacterial or mammalian CFE systems has only been studied in recent years. The microfluidic platform offers an efficient approach for high encapsulation rate with controllable compartment sizes (44–46). In our study, LNA probe in conjunction with a fluorescent reporter protein, and HeLa-based CFE were encapsulated in single-emulsion droplets using a microfluidic device. The microfluidic device was fabricated using conventional soft lithography technique and consisted of two inlet channels, one aqueous channel for CFE and LNA probe, and one oil/surfactant channel. The single emulsions were formed by shearing aqueous solution into a second immiscible solution of mineral oil (in the presence of surfactant Span 80) to generate water-in-oil droplets. The dimensions for the inner phase and outer phase channels were 50 μm in width × 64 μm in height and 80 μm in width × 64 μm in height, respectively (Figure 4A). The generated single-emulsion droplets were collected in a collection channel. Different sizes of single-emulsion droplets ranging from 10 to 200 μm can be generated by adjusting the inner phase and outer phase flow rates. The formed single-emulsion droplets were quite stable and could be easily imaged for up to 24 h. The microfluidic device is robust, easy to implement and could be used repeatedly. All the single-emulsion experiments were conducted using the same microfluidic device to acquire consistent results. Water-in-oil droplets provide an effective method to efficiently reduce

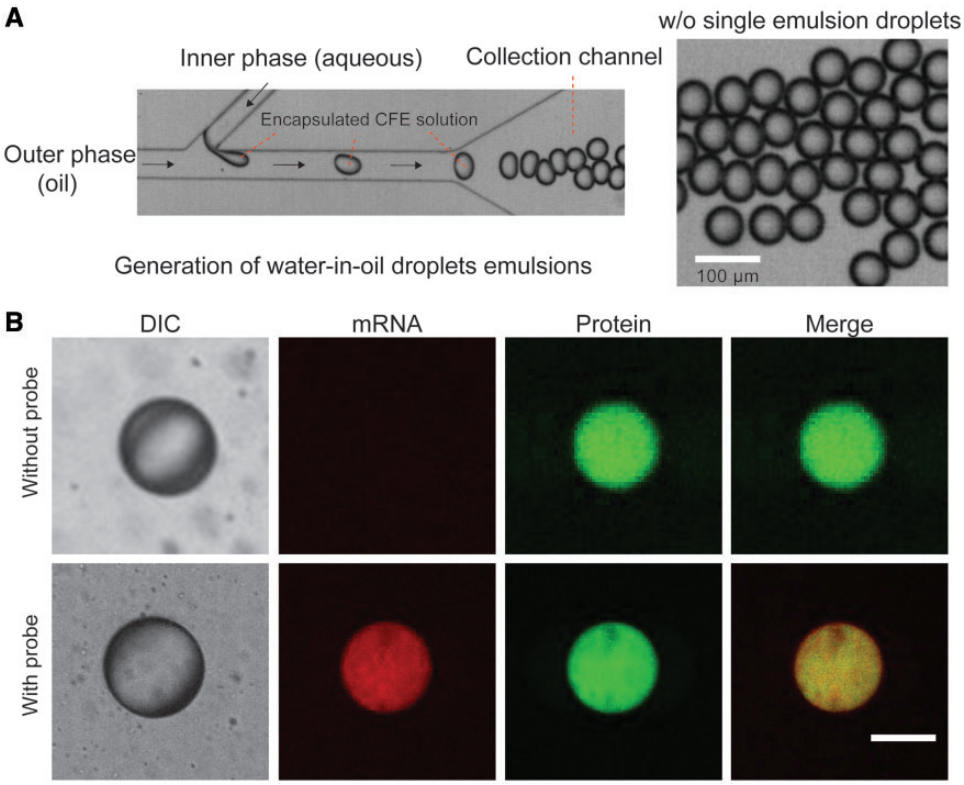

Figure 4. Simultaneous detection of mRNA and protein expression in single-emulsion droplets. (**A**) Generation of water-in-oil single-emulsion droplets using a microfluidic device. The width of inner phase and outer phase channel were 50 and 80 μm, respectively. The formed water-in-oil droplets were stored in the collection channel and collected later by pumping the fluid out. (**B**) Differential interference contrast (DIC) and fluorescence images of a single-emulsion droplet; green color indicates protein expression, and red color indicates mRNA expression. The merged channel shows both mRNA and protein expression in a single-emulsion droplet. The images were acquired after 5 h of incubation at 32°C. Scale bar: 10 μm.

sample volume to picolitre or femtolitre range, compared to the bulk reaction volume of microliters. By encapsulating HeLa-based CFE in picoliter-sized droplets, the TX–TL dynamics were visualized and monitored in the cell-sized droplets.

Before monitoring mRNA and protein expression dynamics over time in single-emulsion droplets, we performed a set of experiments in which droplets were imaged at a single time point (5 h) to confirm the suitability of the LNA probe to visualize mRNA concentration. First, we investigated protein expression without the LNA probe in single-emulsion droplets. Without the LNA probe, GFP can be detected in the green fluorescence channel in a single-emulsion droplet, but corresponding GFP mRNA cannot be detected in the red fluorescence channel, as shown in the top row of Figure 4B. By encapsulating LNA probe together with HeLa-based CFE, the mRNA and protein can be simultaneously detected, as shown in the bottom row of Figure 4B. To demonstrate the specificity of the LNA probe for mRNA detection, the LNA probe and CFE solutions without DNA plasmid were encapsulated to form single-emulsion droplets and imaged in both fluorescence channels. The results showed that there was no green fluorescence detected, as expected, and that the LNA probe had a very low background signal (Supplementary Figure S9).

We next followed mRNA and protein expression dynamics in single-emulsion droplets by encapsulating HeLa-based CFE, DNA plasmid and LNA probe. Fluorescence images of a single-emulsion droplet acquired after 1, 3 and 5 h of incubation allowed for visualization and relative quantification of mRNA and protein expression dynamics over time (Figure 5A). Interestingly, the mRNA level was the highest at the 1-h time point whereas the protein level continued to increase with time. We confirmed this observation by quantifying relative fluorescence intensities corresponding to mRNA and protein levels for multiple droplets of similar sizes (~30 μm) after 1, 3 and 5 h (Figure 5B). Thus, there was an inverse relationship between mRNA and protein levels at these time points, in contrast to a continuous increase of both mRNA and protein during this time points in bulk reactions. This suggests that mRNA and protein expression follow different dynamics in cell-sized droplets compared to bulk reactions. It has been reported that transcription rate is enhanced in membrane-free protocells (47), and protein expression is accelerated in cell-sized confinement in microspheres (48). A difference in bulk versus confined CFE reactions perhaps can be attributed to potential resource limitations due to confinement that has been described for bulk reaction (39) but certainly would play a bigger role with a smaller volume. Meanwhile, Huck and colleagues have shown that crowded environments lead to heterogeneous microenvironments of mRNA expression in picoliter droplets (45). In our experiments, we also observed heterogeneity of mRNA and protein expression in different sized droplets (data not shown). Stochasticity in gene expression of two fluorescence proteins in different sized artificial cells has been investigated and reported (49). However, mRNA levels were not tracked in these experiments. An interesting future direction would be to study gene and protein expression noises in droplets of different sizes as our system is amenable for such investigation given the ability to carry out sequence-dependent detection of different mRNAs.

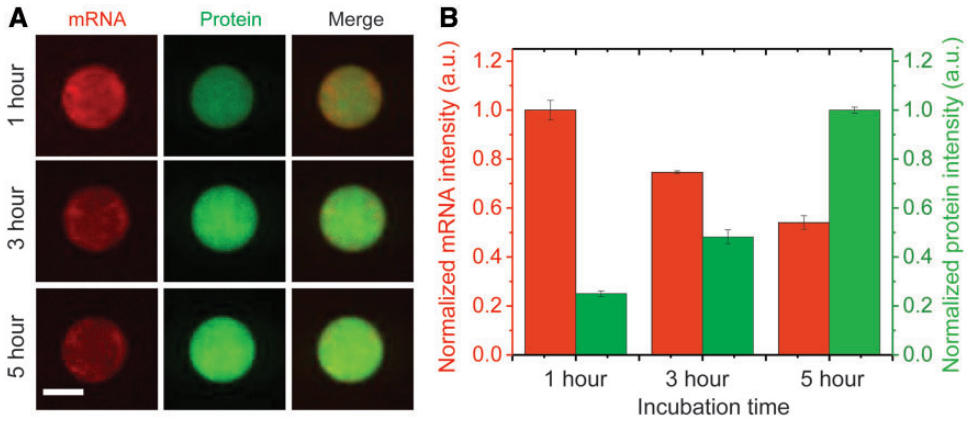

Figure 5. Investigation of mRNA and protein expression dynamics in single-emulsion droplets. (**A**) Simultaneous detection of mRNA and protein expression at different time points in single-emulsion droplets. HeLa-based CFE, DNA plasmid and LNA probe were encapsulated in the droplets. Fluorescence images were acquired at 1, 3 and 5 h of incubation at 32°C. All the images were acquired from the same droplet for comparison. Images were representative images from three independent experiments. Scale bar: 25 μm. (**B**) Mean fluorescence intensity of mRNA and protein expression in single-emulsion droplets at different time points. Experiments were repeated three time independently. Ten droplets of the same size were quantified for each experiment. Data are expressed as mean ± SEM.

In summary, we studied the TX–TL dynamics in HeLa-based CFE in bulk and cell-sized droplets. Our experimental results indicated that this LNA probe is effective in detecting real-time mRNA dynamics with high dynamic range, low background fluorescence, high stability over time and absence of effect on GFP translation. We also characterized the mRNA and protein expression dynamics in CFE and found that TX–TL have distinct dynamics in bulk and in cell-sized droplets. These results show that this LNA probe is an effective tool for studying temporal mRNA dynamics in bulk and in cell-sized droplets, with applications in many areas such as rapid prototyping of mammalian genetic circuits and optimizing the cell-free production of biologics. The effectiveness of this system in cell-sized confinement may also prove useful in understanding and optimizing the dynamics of TX–TL in artificial cells.

SUPPLEMENTARY DATA

Supplementary Data are available at SYNBIO Online.

Acknowledgments

The authors would like to thank Kenneth Ho and Lap Man Lee for the design and fabrication of the microfluidic device for single-emulsion droplet generation.

Funding

The National Science Foundation (NSF) MCB-1612917 and the National Institutes of Health (NIH) Director's New Innovator Award DP2 HL117748-01 to A.P.L.

Conflict of interest statement. None declared.

References

1. Buganim,Y., Faddah,D.A., Cheng,A.W., Itskovich,E., Markoulaki,S., Ganz,K., Klemm,S.L., van Oudenaarden,A. and Jaenisch,R. (2012) Single-cell expression analyses during cellular reprogramming reveal an early stochastic and a late hierarchic phase. *Cell*, 150, 1209–1222.
2. Aymoz,D., Wosika,V., Durandau,E. and Pelet,S. (2016) Real-time quantification of protein expression at the single-cell level via dynamic protein synthesis translocation reporters. *Nat. Commun.*, 7, 11304.
3. Yu,J., Xiao,J., Ren,X., Lao,K. and Xie,X.S. (2006) Probing gene expression in live cells, one protein molecule at a time. *Science*, 311, 1600–1603.
4. Rademacher,A., Erdel,F., Trojanowski,J. and Rippe,K. (2017) Real-time observation of light-controlled transcription in living cells. *J. Cell Sci.*, 130, 4213–4224.
5. Morisaki,T., Lyon,K., DeLuca,K.F., DeLuca,J.G., English,B.P., Zhang,Z., Lavis,L.D., Grimm,J.B., Viswanathan,S., Looger,L.L. et al. (2016) Real-time quantification of single RNA translation dynamics in living cells. *Science*, 352, 1425–1429.
6. Wu,B., Eliscovich,C., Yoon,Y.J. and Singer,R.H. (2016) Translation dynamics of single mRNAs in live cells and neurons. *Science*, 352, 1430–1435.
7. Shimizu,Y., Kuruma,Y., Ying,B.W., Umekage,S. and Ueda,T. (2006) Cell-free translation systems for protein engineering. *FEBS J.*, 273, 4133–4140.
8. Hodgman,C.E. and Jewett,M.C. (2012) Cell-free synthetic biology: thinking outside the cell. *Metab. Eng.*, 14, 261–269.
9. Noireaux,V., Bar-Ziv,R. and Libchaber,A. (2003) Principles of cell-free genetic circuit assembly. *Proc. Natl. Acad. Sci.*, 100, 12672–12677.
10. Garamella,J., Marshall,R., Rustad,M. and Noireaux,V. (2016) The all *E. coli* TX-TL toolbox 2.0: a platform for cell-free synthetic biology. *ACS Synth. Biol.*, 5, 344–355.
11. Shin,J. and Noireaux,V. (2012) An *E. coli* cell-free expression toolbox: application to synthetic gene circuits and artificial cells. *ACS Synth. Biol.*, 1, 29–41.
12. Martin,R.W., Majewska,N.I., Chen,C.X., Albanetti,T.E., Jimenez,R.B.C., Schmelzer,A.E., Jewett,M.C. and Roy,V. (2017) Development of a CHO-based cell-free platform for synthesis of active monoclonal antibodies. *ACS Synth. Biol.*, 6, 1370–1379.
13. Anderson,M.J., Stark,J.C., Hodgman,C.E. and Jewett,M.C. (2015) Energizing eukaryotic cell-free protein synthesis with glucose metabolism. *FEBS Lett.*, 589, 1723–1727.
14. Hansen,M.M., Ventosa Rosquelles,M., Yelleswarapu,M., Maas,R.J., van Vugt-Jonker,A.J., Heus,H.A. and Huck,W.T. (2016) Protein synthesis in coupled and uncoupled cell-free prokaryotic gene expression systems. *ACS Synth. Biol.*, 5, 1433–1440.
15. Villarreal,F. and Tan,C. (2017) Cell-free systems in the new age of synthetic biology. *Front. Chem. Sci. Eng.*, 11, 58–65.

16. Noireaux,V. and Libchaber,A. (2004) A vesicle bioreactor as a step toward an artificial cell assembly. *Proc. Natl. Acad. Sci. USA*, 101, 17669–17674.
17. Thoring,L., Wüstenhagen,D.A., Borowiak,M., Stech,M., Sonnabend,A. and Kubick,S. (2016) Cell-free systems based on CHO cell lysates: optimization strategies, synthesis of "difficult-to-express" proteins and future perspectives. *PLoS One*, 11, e0163670.
18. Brödel,A.K., Sonnabend,A. and Kubick,S. (2014) Cell-free protein expression based on extracts from CHO cells. *Biotechnol. Bioeng.*, 111, 25–36.
19. Mikami,S., Kobayashi,T. and Imataka,H. (2010) Cell-free protein synthesis systems with extracts from cultured human cells. In: Endo Y., Takai K., Ueda T. (eds) *Cell-Free Protein Production. Methods in Molecular Biology (Methods and Protocols)*, vol 607. Humana Press, pp. 43–52.
20. Ho,K.K., Murray,V.L. and Liu,A.P. (2015) Engineering artificial cells by combining HeLa-based cell-free expression and ultrathin double emulsion template. *Methods Cell Biol.*, 128, 303–318.
21. Carlson,E.D., Gan,R., Hodgman,C.E. and Jewett,M.C. (2012) Cell-free protein synthesis: applications come of age. *Biotechnol. Adv.*, 30, 1185–1194.
22. Majumder,S., Garamella,J., Wang,Y.-L., DeNies,M., Noireaux,V. and Liu,A.P. (2017) Cell-sized mechanosensitive and biosensing compartment programmed with DNA. *Chem. Commun.*, 53, 7349–7352.
23. Svensen,N. and Jaffrey,S.R. (2016) Fluorescent RNA aptamers as a tool to study RNA-modifying enzymes. *Cell Chem. Biol.*, 23, 415–425.
24. Filonov,G.S., Moon,J.D., Svensen,N. and Jaffrey,S.R. (2014) Broccoli: rapid selection of an RNA mimic of green fluorescent protein by fluorescence-based selection and directed evolution. *J. Am. Chem. Soc.*, 136, 16299–16308.
25. Rogers,T.A., Andrews,G.E., Jaeger,L. and Grabow,W.W. (2015) Fluorescent monitoring of RNA assembly and processing using the split-spinach aptamer. *ACS Synth. Biol.*, 4, 162–166.
26. Pothoulakis,G., Ceroni,F., Reeve,B. and Ellis,T. (2014) The spinach RNA aptamer as a characterization tool for synthetic biology. *ACS Synth. Biol.*, 3, 182–187.
27. Obernosterer,G., Martinez,J. and Alenius,M. (2007) Locked nucleic acid-based in situ detection of microRNAs in mouse tissue sections. *Nat. Protoc.*, 2, 1508–1514.
28. Wang,S., Sun,J., Xiao,Y., Lu,Y., Zhang,D.D. and Wong,P.K. (2017) Intercellular tension negatively regulates angiogenic sprouting of endothelial tip cells via notch1-Dll4 signaling. *Adv. Biosyst.*, 1, 1600019.
29. ——, Riahi,R., Li,N., Zhang,D.D. and Wong,P.K. (2015) Single cell nanobiosensors for dynamic gene expression profiling in native tissue microenvironments. *Adv. Mater.*, 27, 6034–6038.
30. Niederholtmeyer,H., Xu,L. and Maerkl,S.J. (2013) Real-time mRNA measurement during an in vitro transcription and translation reaction using binary probes. *ACS Synth. Biol.*, 2, 411–417.
31. van Nies,P., Nourian,Z., Kok,M., van Wijk,R., Moeskops,J., Westerlaken,I., Poolman,J.M., Eelkema,R., van Esch,J.H., Kuruma,Y. et al. (2013) Unbiased tracking of the progression of mRNA and protein synthesis in bulk and in liposome-confined reactions. *ChemBioChem*, 14, 1963–1966.
32. ——, Canton,A.S., Nourian,Z. and Danelon,C. (2015) Chapter ten-monitoring mRNA and protein levels in bulk and in model vesicle-based artificial cells. *Methods Enzymol.*, 550, 187–214.
33. Caschera,F., Lee,J.W., Ho,K.K., Liu,A.P. and Jewett,M.C. (2016) Cell-free compartmentalized protein synthesis inside double emulsion templated liposomes with in vitro synthesized and assembled ribosomes. *Chem. Commun.*, 52, 5467–5469.
34. Ho,K.K., Lee,L.M. and Liu,A.P. (2016) Mechanically activated artificial cell by using microfluidics. *Sci. Rep.*, 6, 32912.
35. ——, Lee,J.W., Durand,G., Majumder,S. and Liu,A.P. (2017) Protein aggregation with poly (vinyl) alcohol surfactant reduces double emulsion-encapsulated mammalian cell-free expression. *PLoS One*, 12, e0174689.
36. Hershey,J.W. (1991) Translational control in mammalian cells. *Annu. Rev. Biochem.*, 60, 717–755.
37. Meserve,D., Wang,Z., Zhang,D.D. and Wong,P.K. (2008) A double-stranded molecular probe for homogeneous nucleic acid analysis. *Analyst*, 133, 1013–1019.
38. Schneider-Poetsch,T., Ju,J., Eyler,D.E., Dang,Y., Bhat,S., Merrick,W.C., Green,R., Shen,B. and Liu,J.O. (2010) Inhibition of eukaryotic translation elongation by cycloheximide and lactimidomycin. *Nat. Chem. Biol.*, 6, 209.
39. Siegal-Gaskins,D., Tuza,Z.A., Kim,J., Noireaux,V. and Murray,R.M. (2014) Gene circuit performance characterization and resource usage in a cell-free "breadboard". *ACS Synth. Biol.*, 3, 416–425.
40. Zervantonakis,I.K., Hughes-Alford,S.K., Charest,J.L., Condeelis,J.S., Gertler,F.B. and Kamm,R.D. (2012) Three-dimensional microfluidic model for tumor cell intravasation and endothelial barrier function. *Proc. Natl. Acad. Sci.*, 109, 13515–13520.
41. Sackmann,E.K., Fulton,A.L. and Beebe,D.J. (2014) The present and future role of microfluidics in biomedical research. *Nature*, 507, 181–189.
42. Lee,L.M., Lee,J.W., Chase,D., Gebrezgiabhier,D. and Liu,A.P. (2016) Development of an advanced microfluidic micropipette aspiration device for single cell mechanics studies. *Biomicrofluidics*, 10, 054105.
43. Zheng,Y., Wang,S., Xue,X., Xu,A., Liao,W., Deng,A., Dai,G., Liu,A.P. and Fu,J. (2017) Notch signaling in regulating angiogenesis in a 3D biomimetic environment. *Lab Chip*, 17, 1948.
44. Gach,P.C., Iwai,K., Kim,P.W., Hillson,N.J. and Singh,A.K. (2017) Droplet microfluidics for synthetic biology. *Lab Chip*, 17, 3388.
45. Hansen,M.M., Meijer,L.H., Spruijt,E., Maas,R.J., Rosquelles,M.V., Groen,J., Heus,H.A. and Huck,W.T. (2016) Macromolecular crowding creates heterogeneous environments of gene expression in picolitre droplets. *Nat. Nanotechnol.*, 11, 191–197.
46. Tan,C., Lo,S.-J., LeDuc,P.R. and Cheng,C.-M. (2012) Frontiers of optofluidics in synthetic biology. *Lab Chip*, 12, 3654–3665.
47. Sokolova,E., Spruijt,E., Hansen,M.M., Dubuc,E., Groen,J., Chokkalingam,V., Piruska,A., Heus,H.A. and Huck,W.T. (2013) Enhanced transcription rates in membrane-free protocells formed by coacervation of cell lysate. *Proc. Natl. Acad. Sci. USA*, 110, 11692–11697.
48. Kato,A., Yanagisawa,M., Sato,Y.T., Fujiwara,K. and Yoshikawa,K. (2012) Cell-sized confinement in microspheres accelerates the reaction of gene expression. *Sci. Rep.*, 2, 283.
49. Nishimura,K., Tsuru,S., Suzuki,H. and Yomo,T. (2015) Stochasticity in gene expression in a cell-sized compartment. *ACS Synth. Biol.*, 4, 566–576.